OPEN ACCESS
IOP Publishing
Journal of Physics A: Mathematical and Theoretical
J. Phys. A: Math. Theor. **47** (2014) 395101 (21pp)
doi:10.1088/1751-8113/47/39/395101

Oscillating mushrooms: adiabatic theory for a non-ergodic system

V Gelfreich[1], V Rom-Kedar[2] and D Turaev[3]

[1] Mathematics Institute, University of Warwick, UK
[2] Department of Mathematics, The Weizmann Institute of Science, Israel
[3] Department of Mathematics, Imperial College, London, UK

E-mail: v.gelfreich@warwick.ac.uk, vered.rom-kedar@weizmann.ac.il and dturaev@imperial.ac.uk

Received 28 May 2014, revised 27 July 2014
Accepted for publication 28 July 2014
Published 16 September 2014

Abstract
Can elliptic islands contribute to sustained energy growth as parameters of a Hamiltonian system slowly vary with time? In this paper we show that a mushroom billiard with a periodically oscillating boundary accelerates the particle inside it exponentially fast. We provide an estimate for the rate of acceleration. Our numerical experiments corroborate the theory. We suggest that a similar mechanism applies to general systems with mixed phase space.

Keywords: Fermi acceleration, adiabatic theory, non-autonomous billiards, non-ergodic system

(Some figures may appear in colour only in the online journal)

1. Introduction

Consider a particle which moves freely inside a bounded domain (a billiard) and reflects elastically from the domain's boundary. We assume that the boundary of the billiard changes with time and restores its shape periodically. Elastic collisions with the moving boundary cause changes in the particle kinetic energy. If the average energy gain over multiple collisions is positive, the particle accelerates. This process is often called 'Fermi acceleration' since it resembles the mechanism of cosmic particles acceleration by reflecting from magnetic

mirrors proposed by Fermi in 1949 [14]. In recent years the problem has attracted a lot of attention (see e.g. [4, 5, 12, 13, 16, 22, 25, 30, 35, 36] and references therein).

When the particle accelerates indefinitively, the motion of the boundary eventually becomes slow compared to the particle motion. So we assume that the separation of time scales is already present in the billiard. From the physical point of view, it is important that the motion of the billiard boundary is not affected by the collisions with the particle, i.e. the boundary can be considered as a wall of infinite mass. Thus, the Fermi acceleration can be viewed as a process of energy transfer from a slow heavy object (in our case, the billiard boundary) to fast light particles. In this respect, the crucial question is whether the energy transfer is possible at all, and if so, how effective it is, i.e. what is the rate of the particle energy growth and how it distributes among an ensemble of particles.

We note that there are two alternative approaches to measurements of rates for the Fermi acceleration in billiards. Some authors (e.g. [4, 11, 20, 24, 25]) study the growth of the energy as a function of the collision number n. It is easy to see [16] that the particle speed can grow at most linearly in n. We prefer an alternative point of view, where the billiard is considered as a flow and we study the energy growth with time t. When a particle accelerates the rate of collisions increases, and the resulting energy growth rate may be either polynomial or exponential [15, 18, 26].

It turns out that the acceleration rates strongly depend on the shape of the billiard or, more precisely, on the dynamics of the corresponding 'frozen' billiards. At any given moment of time t, let us stop the slow motion of the billiard boundary. The dynamics within the frozen domain consist of free inertial motion inside the domain and elastic reflections from its static boundary. This standard billiard dynamical system is completely determined by the shape of the frozen domain. Thus, one considers the family of static billiards parameterized by the frozen time t. When all 'frozen' billiards in this family are integrable (e.g. have a rectangular[4], circular or elliptic shape), the papers [11, 20, 24, 25] report either no Fermi acceleration or a slow one. This may be explained by extending the classical adiabatic theory to integrable systems with impacts, as in [19]. On the other hand, if all the frozen billiards are chaotic (e.g. Sinai billiards, Bunimovich stadium, etc), then the Fermi acceleration is usually present [6, 21, 29, 30].

This statement, that chaotic frozen dynamics typically lead to acceleration, is known as the Loskutov–Ryabov–Akinshin conjecture [29] (see also [21]). In a sense, this conjecture was proven in [18] (based on [17]): exponentially accelerating trajectories exist in a billiard of periodically oscillating shape provided every static billiard in the corresponding frozen family has a non-trivial hyperbolic invariant set. The proof uses the existence of a Smale horseshoe structure in the frozen billiards, see also [27]. As a result, the exponentially fast energy growth is established for initial conditions from a set of Lebesgue measure zero only. Such orbits are difficult to observe numerically and, indeed, only power-law energy growth was reported in numerous papers (e.g. [21, 29, 30]). In order to model this moderate growth of the averaged energy seen in numerical experiments, a stochastic differential equation was proposed and verified numerically in [16]. This equation is, in fact, a partial case of the Langevin equation derived in [31]. According to this model the ensemble-averaged Fermi acceleration is quadratic in time, provided all frozen billiards are ergodic and mixing. The slow pace of the acceleration is caused by the long-time preservation of the Anosov–Kasuga adiabatic invariant for a large set of initial conditions [1, 23]. In the billiard context, the Anosov–Kasuga invariant is equal to $EV^{2/d}$, where E is the particle's energy, V is the volume of

[4] The rectangular case reduces to the original one-dimensional Fermi–Ulam model [38] in which no acceleration occurs when the boundary oscillations are smooth in time [33, 34].

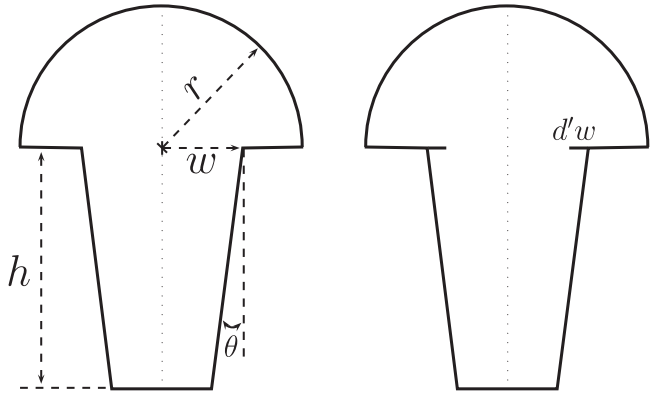

Figure 1. Bunimovich mushrooms.

the billiard and d is the dimension of the billiard domain[5]. For slowly oscillating ergodic billiards, the conservation of the Anosov–Kasuga invariant coincides with the classical thermodynamics adiabatic law for an ideal gas. In particular, the ergodic adiabatic theory predicts that $\frac{E(T)}{E(0)} \approx 1$ for a large set of initial conditions if T is the time-period of oscillations of the billiard shape. In this way the ergodic adiabatic theory prohibits fast acceleration in periodically perturbed ergodic billiards.

A much faster, in fact exponential in time, ensemble-averaged Fermi acceleration is possible when a fraction of the frozen billiard family has several ergodic components [15, 35]. Moreover, in this case most initial conditions experience exponential energy growth. Namely, transitions between different ergodic components of the frozen billiard family lead to a substantial increase in energy transfer to the moving particles.

In this paper we further explore the accelerating effect of the violation of ergodicity: we consider an example of a slow–fast system whose fast subsystem has a chaotic set coexisting with an elliptic island filled by invariant tori. We show that the slow changes in the billiard shape lead to transitions of the fast variables between the chaotic and the elliptic zone of the frozen system. We suggest that these transitions break the Anosov–Kasuga adiabatic conservation law (which can be related to the Boltzmann entropy of the system [16, 31, 36]), cause a systematic increase of the entropy over each period of the slow oscillation, and thus lead to a steady (exponential in time) increase in the energy.

We believe that this general principle of induced exponential acceleration should be applicable to a wide class of slow–fast Hamiltonian systems whose fast subspace contains coexisting chaotic and elliptic components [37]. The recent preprint [5] provides analytical and numerical arguments supporting this conjecture for billiards with mixed phase space, whereas [32] provides numerical evidence for this phenomenon in a smooth system with mixed phase space.

We stress that this conjecture is of great importance as Hamiltonian dynamical systems are rarely ergodic on every energy level. In fact, it is widely believed that the majority of Hamiltonian systems have mixed phase space.

[5] The Anosov–Kasuga theorem is proven only for smooth dynamical systems. Billiard dynamical systems have singularities that correspond to corners and to orbits tangent to the billiard boundary, so the application of the Anosov–Kasuga theory is not formally justified. However, numerical experiments suggest that this theory is still valid for slowly varying billiards [7, 15, 16].

Here we provide a detailed analysis of this process for a special type of a planar billiard with periodically moving boundaries, an oscillating Bunimovich mushroom. The frozen billiard shape is shown in figure 1. This shape was invented in [9]. The corresponding billiard has a phase space that is sharply divided into a single elliptic and a single chaotic component, each one of positive measure [9, 10]. One can easily find explicit expressions for the volumes of the regular and chaotic components. Using this data we propose analytical expressions for the energy distribution after one cycle of the billiard boundary oscillation and predict the energy growth rate. We show that provided the billiard boundary moves along a non-trivial loop in the space of the billiard parameters, a particle inside the billiard accelerates exponentially fast.

Essentially, we show that the process of energy growth over many cycles of boundary oscillations can be modelled by a geometrical Brownian motion, where the particle energy after each cycle is multiplied by an independent random variable. We derive an expression for the expectation of the logarithm of this random factor in terms of the volumes of the chaotic and elliptic components, and show that this expectation is non-negative (and typically strictly positive, which immediately implies the exponential energy growth). Our numerical experiments confirm the predicted growth rate with good precision.

The paper has the following structure. In section 2 we study the properties of the Bunimovich mushroom [9] and find explicit expressions for the volumes of the regular and chaotic components. Section 3 contains our main theoretical results. In particular, we derive an adiabatic theory in the presence of particle flux, which is used to calculate the change in the particle's energy while it stays in the chaotic or regular component. Then we find the probability of capture into the regular component. Finally, we calculate the averaged growth rate of energy over a period of the mushroom oscillations, and show that this rate is non-negative. Moreover, it is strictly positive for generic oscillations. Thus the average energy increases exponentially fast. In section 4 we present several numerical experiments that confirm our prediction for the energy growth rate, probabilities of capture into the elliptic island and distributions of the energy. In section 5 we summarise the work and discuss possible extensions for our theory.

2. Frozen mushroom

A Bunimovich mushroom consists of a semi-disk and a stem [9] (see figure 1). A particle moves freely inside the mushroom D and reflects elastically from its boundary. The particle can go from the cap to the stem and back through a hole. The dynamics of the particle are defined by the Hamiltonian

$$H(\mathbf{p}, \mathbf{x}) = \frac{p_x^2 + p_y^2}{2} \qquad \text{for } \mathbf{x} \in D,$$

where $\mathbf{p} = (p_x, p_y)$ and $\mathbf{x} = (x, y)$ are respectively the momentum and position of the particle. On the boundary of D the particle velocity is reflected according to the elastic low: the incidence angle is equal to the reflection angle and the absolute value of the velocity is not changed.

The phase space of the Bunimovich mushroom consists of two invariant components of positive Lebesgue measure: a regular component (an elliptic island) filled by invariant tori, and a chaotic component, which is ergodic and mixing [9, 10]. The regular component consists of points trapped in the mushroom cap.

Let r and w denote the radius of the cap and the semi-width of the hole respectively (see figure 1 (left)). When the particle moves inside the cap, the incidence angle φ with the semi-circular part of the boundary remains constant. So if at some collision

$$|\sin\varphi| \geqslant \nu = \frac{w}{r},$$

the particle cannot reach the hole and consequently never leaves the cap. Along these trajectories the absolute value of the angular momentum, $|xp_y - yp_x|$, is preserved, and consequently the dynamics are integrable. The chaotic component is the complement to the integrable one [10].

In this paper we will consider a tilted Bunimovich mushroom in the domain $D = D_{\text{stem}} \cup D_{\text{cap}}$ defined by

$$\begin{aligned} D_{\text{stem}} &= \{\, |x| \leqslant w + y\tan\theta \quad \text{and} \quad -h \leqslant y \leqslant 0 \,\}, \\ D_{\text{cap}} &= \left\{\, x^2 + y^2 \leqslant r \text{ and } y \geqslant 0 \,\right\}. \end{aligned}$$

We assume that $w \leqslant r$ and $|\theta| < \frac{\pi}{2}$. For simplicity of presentation we assume that for positive θ the cone extends up to $y = h$, namely, that $w \geqslant h\tan\theta$. At $\theta = 0$ we obtain the original Bunimovich mushroom (which has a family of parabolic orbits formed by horizontal oscillations inside the stem, whereas at non-zero θ the family of parabolic orbits is destroyed). It can be shown by methods of [8, 10] that the tilted mushroom has, for every θ, the same property as the non-tilted one: the complement to the set of points whose orbits are forever trapped in the cap is ergodic and mixing.

Consider a set $D_0 \subset D \subset \mathbb{R}^2$ and let $A(D_0)$ denote its area. Let $V(D_0)$ be the phase space volume of the set defined by $H(x, y, p_x, p_y) = \frac{1}{2}$ and $(x, y) \in D_0$. Obviously, the volume of all points in the phase space such that $H(x, y, p_x, p_y) = E$ and $(x, y) \in D_0$ is equal to $2\pi\sqrt{2E}A(D_0)$, so $V(D_0) = 2\pi A(D_0)$.

In particular, we find that

$$V_{\text{cap}} = \pi^2 r^2 \qquad \text{and} \qquad V_{\text{stem}} = 2\pi\Big(2wh - h^2\tan\theta\Big). \tag{1}$$

For the future analysis we will need to find volumes of the integrable and chaotic components. The elliptic island (i.e., the integrable component) occupies only a part of the cap. Let V_{ell} be the phase space volume of the elliptic island at the energy level $H = \frac{1}{2}$. We claim that

$$V_{\text{ell}} = \delta(\nu)V_{\text{cap}}(r), \tag{2}$$

where $\nu = \frac{w}{r}$ and

$$\delta(\nu) = 2\pi^{-1}\Big(\arccos\nu - \nu\sqrt{1-\nu^2}\Big). \tag{3}$$

Indeed, consider a point $(x, y) = (\rho\cos\psi, \rho\sin\psi)$ inside the cap with a velocity vector (p_x, p_y). Then define the angle ϕ by $(p_x, p_y) = (v\cos(\psi - \phi), v\sin(\psi - \phi))$, where $v = \sqrt{2E}$. The absolute value of angular momentum is equal to $v\rho|\sin\phi|$. Notice that at the cap boundary the angle ϕ coincides with the incidence angle φ. The integrable component consists of trajectories that never cross the stem-cap boundary $\{\psi = 0, \rho < w\} \cup \{\psi = \pi, \rho < w\}$, where w is the half width of the hole. Since the angular momentum is conserved, and it is smaller than wv on this boundary, the integrable component at $v = 1$ is defined by the inequalities

$$\mathcal{D}_{\rm ell} := \left\{ \frac{w}{|\sin\phi|} \leqslant \rho \leqslant r, \quad 0 \leqslant \psi \leqslant \pi, \quad 0 \leqslant \phi \leqslant 2\pi \right\}. \tag{4}$$

Introducing $s_1 = \rho\cos\varphi$, $s_2 = \rho\sin\varphi$, we get

$$\mathcal{D}_{\rm ell} = \left\{ s_1^2 + s_2^2 \leqslant r^2, \quad |s_2| \geqslant w, \quad 0 \leqslant \psi \leqslant \pi \right\},$$

so the volume is given by the following integral

$$V_{\rm ell} = \int_{\mathcal{D}_{\rm ell}} \mathrm{d}s_1\, \mathrm{d}s_2\, \mathrm{d}\psi = 4\pi \int_w^r \sqrt{r^2 - s_2^2}\, \mathrm{d}s_2.$$

Dividing by $V_{\rm cap}$ and using (1), we obtain (2).

The chaotic component is the complement of the regular one, therefore its volume is given by

$$V_{\rm cha} = V_{\rm cap} + V_{\rm stem} - V_{\rm ell}. \tag{5}$$

3. Adiabatic oscillations and capture into an island

Now suppose that the parameters of the mushroom change slowly with time. The speed of the particle is no longer preserved and we study the time evolution of the particle's energy. The classical adiabatic theory describes dynamics for a slowly changing integrable system [2, 3, 28], and the ergodic adiabatic theory studies the case when the system is ergodic at every energy level for every frozen moment of time [1, 23]. Neither of these theories is directly applicable when the phase space of the frozen system is a mixture of integrable and chaotic components as the particle can transfer from one type of motion to another one due to the changes in the system.

3.1. Dynamics in an oscillating circular billiard

While the particle stays in the cap, its dynamics can be described by a circular billiard of the same radius. We assume that the radius is a given smooth function of time, $r(t)$, and the centre of the circle does not move. Let the particle hit the boundary at a point P and φ be the impact angle, i.e., the angle between the pre-collision velocity and the external normal to the boundary at the point of collision. Let $v_\parallel = v\sin\varphi$ denote the component of the particle velocity parallel to the boundary, and $v_\perp = v\cos\varphi$ be the normal component of the velocity. The elastic reflection $(v_\parallel, v_\perp) \mapsto (\bar v_\parallel, \bar v_\perp)$ from the moving boundary is given by

$$\bar v_\parallel = v_\parallel, \qquad \bar v_\perp = 2u(t) - v_\perp,$$

where $u(t) = \dot r(t)$ is the velocity of the boundary motion (note that the relation $\bar v_\perp - u(t) = -(v_\perp - u(t))$ represents the standard elastic law in the coordinate frame that moves with the boundary). Then for the outgoing angle $\bar\varphi$ we have $\tan\bar\varphi = \frac{\sin\varphi}{\cos\varphi - 2\frac{u}{v}}$ and consequently

$$\bar\varphi = \varphi + 2\frac{u(t)}{v}\sin\varphi + O\left(v^{-2}\right). \tag{6}$$

We assume that the particle moves much faster than the boundary, i.e. $u \ll v$. The particle speed after the collision is given by

$$\bar{v} = \sqrt{\bar{v}_{\parallel}^2 + \bar{v}_{\perp}^2} = v\left(1 - 2\frac{u}{v}\cos\varphi + O\left(v^{-2}\right)\right).$$

The time interval Δt to the next collision is $L\bar{v}^{-1}$ where $L = |PQ|$ is the distance to the next collision point Q. Since $\Delta t = O(v^{-1})$, the change in the circle radius is also $O(v^{-1})$, so L is $O(v^{-1})$-close to the value it takes in the static circular billiard of radius $r(t)$, i.e. to the length of the chord that makes the angle φ to the radius. This gives us

$$\Delta t = \frac{2r\cos\varphi}{v} + O\left(v^{-2}\right).$$

The new value of the radius at the moment of the next collision is

$$r' = r(t + \Delta t) = r(t)\left(1 + 2\frac{u(t)\cos\varphi}{v}\right) + O\left(v^{-2}\right). \tag{7}$$

Now, by considering the triangle PQO where O is the centre of the circle, we find

$$\frac{r(t)}{\sin\varphi'} = \frac{r'}{\sin\bar{\varphi}},$$

where φ' is the impact angle at the collision point Q. By (6), (7), we obtain

$$\varphi' = \varphi + O\left(v^{-2}\right). \tag{8}$$

It follows immediately that the impact angle φ stays approximately constant over time required for at least $O(v)$ collisions, i.e. φ is an adiabatic invariant.

Since the circular billiard keeps being rotationally symmetric even when its radius oscillates, the angular momentum is preserved

$$v'r'\sin\varphi' = vr\sin\varphi.$$

Taking into account equation (8) we conclude that

$$v'r' = vr\left(1 + O\left(v^{-2}\right)\right).$$

It follows immediately that the product $v(t)r(t)$ stays approximately constant over time required for $O(v)$ collisions. Taking the square, we see that $E(t)V_{\mathrm{cap}}(t)$ is an adiabatic invariant.

In terms of the billiard flow, the adiabatic invariance of the impact angle φ can be expressed as the adiabatic invariance of the angle $\hat{\varphi}$ defined as

$$\sin\hat{\varphi} = -\frac{xp_y - yp_x}{\sqrt{2E}\,r(t)}. \tag{9}$$

Indeed, at the moments of collision $\hat{\varphi}$ coincides with φ, and it stays approximately constant between impacts. In the oscillating mushroom the above equations are valid for segments of trajectories located entirely inside the mushroom cap.

3.2. Capturing into the cap

Suppose that a fast particle moves inside the non-autonomous mushroom. While the particle moves inside the mushroom cap, its dynamics follow the laws of the circular billiard but the sign of its angular momentum is reflected each time the particle hits the bottom of the cap. The hole of the mushroom cap is characterized by the dimensionless parameter

$$\nu(t) = \frac{w(t)}{r(t)}. \tag{10}$$

Suppose that at a moment $t = t_0$ the particle is exactly at the hole. Then it is located at a point $(x, 0)$ with $|x| < w(t_0)$ and has velocity (p_x, p_y). Let $\sin\varphi_0 = |\sin\hat{\varphi}(t_0)|$ be the absolute value of the adiabatic invariant defined by equation (9). Since $|p_y| \leqslant \sqrt{2E}$ we conclude that $\sin\varphi_0 \leqslant \nu(t_0)$.

If at this moment $p_y > 0$, the particle enters the cap and can have multiple consecutive collisions inside the cap. We have already seen that $|\sin\hat{\varphi}(t)|$ is adiabatically invariant while the particle stays inside the cap. So if the function ν decreases below $\sin\varphi_0$ while the particle remains inside the cap, the particle cannot reach the hole. So it must remain in the cap till ν returns back to $\sin\varphi_0$.

We see that the particle can be captured into the cap when ν decreases. If the particle is captured at $t = t_{\text{in}}$, then it is released back into the chaotic zone around the moment $t = t_{\text{out}}$ when $\nu(t_{\text{out}}) = \nu(t_{\text{in}})$ for the first time. Thus, we can introduce the release function $t_r(t)$

$$t_r(t) = \inf\left\{t' \colon t' > t \text{ and } \nu(t') \geqslant \nu(t)\right\}, \tag{11}$$

which establishes a connection between the capture and release times as $t_{\text{out}} = t_r(t_{\text{in}})$.

3.3. Adiabatic theory in the presence of particle flux

The classical ergodic adiabatic theory [1, 7, 23] relies on the analysis of evolution of volumes in the phase space. This theory relies on two observations which can be presented in a bit oversimplified form in the following way. First, the ergodicity implies that time averages can be replaced by space averages and, consequently, the time evolution of the energy is the same for the majority of initial conditions starting on a given energy level. Second, if the evolution of the energy depended on initial energy only, the dynamics would map an energy level into another energy level. Since the Hamiltonian flow is volume preserving, the volume under the energy level would stay constant. In a two-dimensional billiard this volume is proportional to EV, which is indeed the ergodic adiabatic invariant.

If the system is not ergodic on energy levels, the dynamics may produce phase space flux between different ergodic components of the frozen system. Then, the above volume preservation argument is invalid. A new paradigm is thus developed.

In the non-autonomous mushroom billiard the flux between the regular and chaotic zones is governed by the parameter $\nu(t)$ defined by (10). If $\dot{\nu} < 0$, phase volume 'leaks' from the chaotic zone to the regular one, whereas $\dot{\nu} > 0$ leads to the opposite effect.

We analyze this situation by considering a short time interval, $[t, t + \mathrm{d}t]$, at which the mushroom's shape does not change noticeably, yet, the particle experiences a large number of collisions with the billiard boundary. Suppose that during this time interval the radius of the hole w has changed by $\mathrm{d}w$, the length of the stem h has changed by $\mathrm{d}h$ and the radius of the cap r has changed by $\mathrm{d}r$.

In this discussion we need to distinguish two cases depending on the sign of

$$\mathrm{d}\nu = \frac{r\mathrm{d}w - w\mathrm{d}r}{r^2}, \tag{12}$$

which determines the direction of the particle flux between the integrable and chaotic components. In particular, if $r\mathrm{d}w < w\mathrm{d}r$, the particle in the integrable component cannot leave the cap but the particle in the chaotic zone can be captured into the integrable component. Let us consider the case of capture, $\mathrm{d}\nu < 0$, in more details.

We conjecture that if the particle is sufficiently fast and the changes in the billiard's shape are sufficiently small then, from the statistical point of view, the distribution of the energies at $t + \mathrm{d}t$ depends only on the initial and final billiard shapes, i.e., it depends only on the values of $\mathrm{d}w$, $\mathrm{d}h$, $\mathrm{d}r$ and $\mathrm{d}\theta$, and is independent of the particular form of the evolution of the billiard's shape in the intermediate moments of time.

Now, in order to separate the process of capturing into the cap from the adiabatic evolution of the energy, we represent the change of the billiard's shape as a composition of two steps. At the first step, we allow the mushroom to take the intermediate shape shown on figure 1 (right): we make the hole in the cap slightly narrower by inserting two straight-line segments into the hole that symmetrically extend the cup bottom line.

We use the notation $\mathrm{d}'z$ and $\mathrm{d}''z$ to label changes of a parameter z during the first and second of these steps respectively ($z \in \{r, w, h, \theta\}$). So, over the time interval $\mathrm{d}t$ we get $\mathrm{d}z = \mathrm{d}'z + \mathrm{d}''z$.

The shape of the billiard at the end of stage 1 is uniquely defined by the following requirements: on stage 1 the particle energy is not changed but all possible transitions between the chaotic and integrable component take place during this step, i.e., $\mathrm{d}'E = 0$ and $\mathrm{d}'\nu = \mathrm{d}\nu < 0$. On stage 2 the particle cannot move from the integrable to the chaotic component or vice versa. This condition is achieved by the requirement $\mathrm{d}''\nu = 0$. All changes in the energy are on this step: $\mathrm{d}E = \mathrm{d}''E$.

On stage 1 all walls remain static (hence $\mathrm{d}'h = 0$, $\mathrm{d}'\theta = 0$, $\mathrm{d}'r = 0$) except for the bottom of the cap, which extends to cover a part of the hole as shown on figure 1 (right). By the end of this stage the radius of the hole is changed by

$$\mathrm{d}'w = r\mathrm{d}\nu,$$

which is negative since we assume $\mathrm{d}\nu < 0$. Moreover, the parameter ν takes its final value

$$\mathrm{d}'\nu = \mathrm{d}\nu.$$

The total volume of the phase space remains constant on this stage but a part of the phase volume is transferred from the chaotic to the regular component

$$\mathrm{d}'V_{\mathrm{cha}} + \mathrm{d}'V_{\mathrm{ell}} = 0, \qquad \mathrm{d}'V_{\mathrm{ell}} = V_{\mathrm{cap}}\ \mathrm{d}\delta. \tag{13}$$

The last equality is a consequence of equation (2) and the requirement $\mathrm{d}'r = 0$. It is important to note that on stage 1 the energy remains constant. Indeed, as the straight-line segments that are inserted into the hole slide along themselves, and the other parts of the billiard boundary do not move during the stage 1, the normal velocity of the boundary is non-zero only at two points, the end points of these two segments. Therefore, the particle energy can change only if it hits the boundary exactly at one of these points at some moment of time, but this is a probability zero event.

On stage 2 the billiard is slowly deformed from its intermediate shape to the final one in such a way that the parameter $\nu = \frac{w}{r}$ remains constant, $\mathrm{d}''r = \mathrm{d}r$ and $\mathrm{d}''\nu = 0$. Then equation (12) implies that $\mathrm{d}'w + \mathrm{d}''w$ attains its correct final value $\mathrm{d}w$. At the same time h, θ are changed to ensure $\mathrm{d}''h = \mathrm{d}h$, $\mathrm{d}''\theta = \mathrm{d}\theta$. It follows that on stage 2 the particle is trapped either in the regular or in the chaotic zone and cannot transfer from one component to the other due to the conservation of impact angles in the circular part.

If the particle is in the regular zone, its dynamics are described by the circular billiard and its energy changes according to the adiabatic law $\mathrm{d}''(EV_{\mathrm{cap}}) = 0$ as derived in section 3.1. Since both E and V_{cap} are constant on stage 1, and we get $\mathrm{d}E = \mathrm{d}''E$, $\mathrm{d}V_{\mathrm{cap}} = \mathrm{d}''V_{\mathrm{cap}}$ and, consequently

$$\frac{\mathrm{d}E}{E} = -\frac{\mathrm{d}V_{\mathrm{cap}}}{V_{\mathrm{cap}}}. \tag{14}$$

Since the flux is absent the chaotic zone remains invariant for the non-autonomous billiard, and we assume that the standard ergodic adiabatic theory can be applied to the restriction of our dynamical system onto its invariant subset. So if the particle is inside the chaotic zone, then the absence of flux allows us to claim that $\mathrm{d}''(EV_{\mathrm{cha}}) = 0$. Using equation (13) we get

$$\mathrm{d}''V_{\mathrm{cha}} = \mathrm{d}V_{\mathrm{cha}} - \mathrm{d}'V_{\mathrm{cha}} = \mathrm{d}V_{\mathrm{cha}} + \mathrm{d}'V_{\mathrm{ell}} = \mathrm{d}V_{\mathrm{cha}} + V_{\mathrm{cap}}\ \mathrm{d}\delta.$$

Since $\mathrm{d}''E = \mathrm{d}E$, we conclude that for particles in the chaotic zone

$$\frac{\mathrm{d}E}{E} = -\frac{\mathrm{d}V_{\mathrm{cha}}}{V_{\mathrm{cha}}} - V_{\mathrm{cap}}\frac{\mathrm{d}\delta}{V_{\mathrm{cha}}}, \tag{15}$$

where V_{cha} is given by (5). Note that in contrast with the classical ergodic adiabatic theory, the right-hand side of this equality contains an additional term which takes care of the phase volume flux from the chaotic zone.

One can check that the same equations describe the evolution of the energy in the case when $\mathrm{d}\nu > 0$ (flux from the integrable to chaotic component). The equations can be derived in a similar way but stages 1 and 2 are to be swapped.

3.4. Probability of capture

In order to describe the acceleration induced by the capture-release mechanism we consider an ensemble of non-interacting particles inside the billiard. Then we can discuss the probabilities for a particle to be captured inside the mushroom cap.

Suppose that $\dot{\nu} \leqslant 0$ on a time interval (t_0, t_1) so the quotient $\nu(t) = w(t)/r(t)$ is decreasing. We start with $n_{\mathrm{cha}}(t_0)$ particles with initial conditions uniformly distributed inside the chaotic zone. We assume that the distribution of the particles in the chaotic zone remains uniform for all times.

Let $t \in [t_0, t_1)$. We consider the transfer of particles from the chaotic zone during the time interval $(t, t + \mathrm{d}t)$ following the two-steps approximation described in the previous section. On Stage 1, a volume of size

$$\mathrm{d}'V_{\mathrm{ell}} = V_{\mathrm{cap}}\ \mathrm{d}\delta$$

is transferred from the chaotic zone to the regular component, and on stage 2 the number of particles in the chaotic zone remains unchanged. Since the particles are uniformly distributed we get

$$\frac{\mathrm{d}n_{\mathrm{cha}}}{n_{\mathrm{cha}}} = -\frac{V_{\mathrm{cap}}\ \mathrm{d}\delta}{V_{\mathrm{cha}}}.$$

Let $p_{\mathrm{cha}}(t) = n_{\mathrm{cha}}(t)/n_{\mathrm{cha}}(t_0)$ be the probability of being in the chaotic zone at the time t. On the time interval (t_0, t_1), the function p_{cha} satisfies the relation

$$\frac{\mathrm{d}p_{\mathrm{cha}}}{p_{\mathrm{cha}}} = \frac{\mathrm{d}n_{\mathrm{cha}}}{n_{\mathrm{cha}}} = -\frac{V_{\mathrm{cap}}}{V_{\mathrm{cha}}}\ \mathrm{d}\delta. \tag{16}$$

Integrating equation (16) we get

$$p_{\rm cha}(t) = p_{\rm cha}(t_0)\exp\left(-\int_{t_0}^{t} \frac{V_{\rm cap}}{V_{\rm cha}}\, {\rm d}\delta \right) \tag{17}$$

for all $t \in (t_0, t_1)$. We stress that these equations are valid only during the period of capture when no particles are released from the elliptic zone.

3.5. Energy growth rate over a cycle

Suppose that the parameters of the mushroom are periodic functions of time and let T be the period. During this cycle a particle from the chaotic zone may be captured into the island when $\nu(t)$ decreases. If the particle is captured at a time t, then it is released at the time $t_r(t)$ defined by (11). Note that according to this definition, if $\nu(t)$ is increasing at some t, then $t_r(t) = t$. We also note that $\nu(t) = \nu(t_r(t))$. Since all particles captured between t and $t_r(t)$ are released back into the chaotic zone by the time $t_r(t)$, we also get $n_{\rm cha}(t) = n_{\rm cha}(t_r(t))$ for all t. We assume that at $t = 0$ the parameter $\nu(t)$ takes its maximum, so all particles which were captured inside the chaotic zone during the cycle are releases back by the beginning of the next cycle.

Let us define a compression factor which describes the change in the relative size of the chaotic zone during the time of capture

$$g(t) = \frac{V_{\rm cha}(t)}{V_{\rm cap}(t)} \Big/ \frac{V_{\rm cha}\big(t_r(t)\big)}{V_{\rm cap}\big(t_r(t)\big)}. \tag{18}$$

Let $S(t) = \log E(t)$ and $\mathbb{S}(t) = \mathbb{E}[S(t)]$. Then equations (14) and (15) imply that

$${\rm d}S = \begin{cases} -\dfrac{{\rm d}V_{\rm cha}}{V_{\rm cha}} - V_{\rm cap}\dfrac{{\rm d}\delta}{V_{\rm cha}} & \text{inside the chaotic zone,} \\ -\dfrac{{\rm d}V_{\rm cap}}{V_{\rm cap}} & \text{in the island.} \end{cases} \tag{19}$$

The total number of particles is $n_0 = n_{\rm cha} + n_{\rm ell}$. Consequently,

$${\rm d}\mathbb{S} = \frac{n_{\rm cha}}{n_0}\left(-\frac{{\rm d}V_{\rm cha}}{V_{\rm cha}} - V_{\rm cap}\frac{{\rm d}\delta}{V_{\rm cha}} \right) - \left(1 - \frac{n_{\rm cha}}{n_0} \right)\frac{{\rm d}V_{\rm cap}}{V_{\rm cap}},$$

We can rewrite this equation in the following form

$${\rm d}\mathbb{S} = -\frac{n_{\rm cha}}{n_0}{\rm dlog}\left(\frac{V_{\rm cha}}{V_{\rm cap}} \right) - \frac{n_{\rm cha}}{n_0}\frac{V_{\rm cap}}{V_{\rm cha}}{\rm d}\delta - {\rm dlog}V_{cap}.$$

Integrating over a complete cycle and taking into account that $p_{\rm cha} = n_{\rm cha}/n_0$ (all particles are in the chaotic zone at the beginning) we get

$$\mathbb{S}(T) - \mathbb{S}(0) = \int_0^T {\rm d}\mathbb{S}(t) = -\int_0^T p_{\rm cha}\,{\rm dlog}\left(\frac{V_{\rm cha}}{V_{\rm cap}} \right) - \int_0^T p_{\rm cha}\frac{V_{\rm cap}}{V_{\rm cha}}\,{\rm d}\delta.$$

The first term may be integrated by parts

$$I_1 = -\int_0^T p_{\rm cha}\,{\rm d}\log\left(\frac{V_{\rm cha}}{V_{\rm cap}}\right) = \int_0^T \log\left(\frac{V_{\rm cha}}{V_{\rm cap}}\right){\rm d}p_{\rm cha} = \int_{\rm capture} \log g(t)\,{\rm d}p_{\rm cha},$$

where we grouped together contributions from capture-release pairs taking into account that $p_{\rm cha}(t) = p_{\rm cha}(t_r(t))$ and $\delta(t) = \delta(t_r(t))$. For the second integral we get

$$\begin{aligned} I_2 = & -\int_0^T p_{\rm cha}\frac{V_{\rm cap}}{V_{\rm cha}}\,{\rm d}\delta = -\int_{\rm capture} p_{cha}(t)\left(\frac{V_{\rm cap}(t)}{V_{\rm cha}(t)} - \frac{V_{\rm cap}(t_r)}{V_{\rm cha}(t_r)}\right){\rm d}\delta(t) \\ = & -\int_{\rm capture} p_{\rm cha}(t)(1-g(t))\frac{V_{\rm cap}(t)}{V_{\rm cha}(t)}{\rm d}\delta(t) = \int_{\rm capture}(1-g(t)){\rm d}p_{\rm cha}, \end{aligned}$$

where we used equation (16) which is valid during the capture process. Defining $p_{\rm ell} = 1 - p_{\rm cha}$ we get the formula

$$m_1 := \mathbb{E}\left[\log\frac{E(T)}{E(0)}\right] = \mathbb{S}(T) - \mathbb{S}(0) = \int_{\rm capture}(g - 1 - \log g){\rm d}p_{\rm ell}. \qquad (20)$$

Since $p_{\rm ell}(t)$ is a non-decreasing function of time during the capture and $\log g < g - 1$ for any $g > 0$, $g \neq 1$, we conclude that the energy growth rate m_1 is non-negative. Moreover, it is strictly positive if $g(t) \not\equiv 1$. As $p_{\rm ell}$ increases during the capture process, we have shown that

$$\mathbb{E}\left[\log\frac{E(T)}{E(0)}\right] > 0$$

for any periodic cycle which is non-trivial, namely, for any cycle having a non-trivial interval of capture with $g(t) \not\equiv 1$ on this interval.

Since $\nu(t) = \nu(t_r(t))$ and δ is a function of ν only, we get $\delta(\nu(t)) = \delta(\nu(t_r(t)))$, i.e., at the moments of capture and release, the regular zone takes the same proportion of the cap's phase space volume. We conclude that $g(t) = 1$ if and only if $V_{\rm cap}(t)/V_{\rm stem}(t) = V_{\rm cap}(t_r)/V_{\rm stem}(t_r)$ (see (18), (5)).

This observation can be restated in the following way. The equation $\left(\frac{V_{\rm ell}(t)}{V_{\rm cap}(t)}, \frac{V_{\rm cap}(t)}{V(t)}\right)$ with $t \in (0, T)$ defines a closed curve. If this curve encloses a non-empty interior, the cycle is non-trivial. On the other hand, any cycle with an empty interior is trivial. In particular, if one changes only a single parameter of the billiard, the above mechanism does not produce the exponential acceleration and we expect much slower acceleration rates.

Next, we assume that all particles have the same energy $E(0)$ at the beginning of the billiard cycle and derive an equation for the energy distribution at the end of the cycle. For simplicity we assume that the billiard cycle contains a single interval of capture, i.e. $\dot\nu$ is negative only on a single interval of time during one complete cycle of the billiard boundary. Then each particle can be captured at most once per billiard cycle. Suppose that a particle is captured at $t = t_{\rm in}$ and let $E_1(t_{\rm in})$ be its energy at the end of the cycle. In the adiabatic approximation its energy can be obtained by integrating equation (19)

$$\log\frac{E_1(t_{\rm in})}{E_0} = \int_{[0,t_{\rm in}]\cup[t_{\rm out},T]}\left(-\frac{{\rm d}V_{\rm cha}}{V_{\rm cha}} - V_{\rm cap}\frac{{\rm d}\delta}{V_{\rm cha}}\right) - \int_{t_{\rm in}}^{t_{\rm out}}\frac{{\rm d}V_{\rm cap}}{V_{\rm cap}}$$
$$= -\log g(t_{\rm in}) + \int_{t_{\rm out}}^{t_{\rm in}+T}\left(-V_{\rm cap}\frac{{\rm d}\delta}{V_{\rm cha}}\right), \qquad (21)$$

where the second line uses the definition of the compression factor (equation (18)) and the fact that $\int_0^T {\rm d}(\log V_{\rm cha}) = 0$. Since the probability of capture at $t \in [t_{\rm in},\, t_{\rm in} + {\rm d}t_{\rm in}]$ is equal to $-\dot{p}_{\rm cha}(t_{\rm in}){\rm d}t_{\rm in}$ where $p_{\rm cha}$ is given by equation (17), we obtain the probability distribution of the energy after the cycle in an implicit form. Later in this paper we will use these implicit equations to reconstruct the distribution of the energy for specific examples of the mushroom cycles.

On the other hand, if the particle is not captured over the cycle its energy is defined in the adiabatic approximation (see (15))

$$\log\frac{E_1^{nc}}{E_0} = \int_0^T\left(-\frac{{\rm d}V_{\rm cha}}{V_{\rm cha}} - V_{\rm cap}\frac{{\rm d}\delta}{V_{\rm cha}}\right) = -\int_0^T V_{\rm cap}\frac{{\rm d}\delta}{V_{\rm cha}}. \qquad (22)$$

This equation implies that, if the particle stays in the chaotic zone over the whole cycle, its energy at the end of the cycle does not need to be equal to the initial energy. This conclusion is in a strong contrast with the ergodic case, where the adiabatic theory predicts that the energy returns close to its initial value at the end of a cycle. The changes in the energy are determined solely by the correction term in (15), which takes into account the phase flux due to the non-ergodicity of the frozen billiards. So the phase flux influences the evolution of the energy even for the particles which never cross to the regular zone.

Any closed curve in the space of parameters defines two billiard cycles which correspond to two different directions of motion along the curve. The values of the integrals (22) for these two cycles have the same absolute value but opposite signs. So the energy of the non-captured particles may increase or decrease after the completion of the cycle, but in both cases the energy averaged over all initial conditions increases.

In the next section we check numerically the prediction of equation (22) for several examples of billiard cycles.

4. Examples of billiard cycles

The theory developed in the previous sections relies upon several assumptions, which are difficult to prove analytically. In particular, we assume that the ergodic averaging theory is applicable to the chaotic component in a system which does not satisfy some of the assumptions of the original averaging theory. The most dramatic violation here is that there are transitions between the ergodic components—we propose that formula (15) replaces the usual adiabatic law. Additionally, the billiard is not a smooth system (see discussion in [16]). Finally, we also assume here that the distribution of the particle in the chaotic zone of the breathing billiard is close to the stationary uniform one. So we carry out numerical tests to check the correctness of the theoretical predictions for the energy growth rate and for the distribution of the energy after a cycle of the billiard boundary.

4.1. Fixed cap

Our first example corresponds to the following protocol for the time dependence of the mushroom parameters: the radius of the gap and the length of the stem follow straight lines

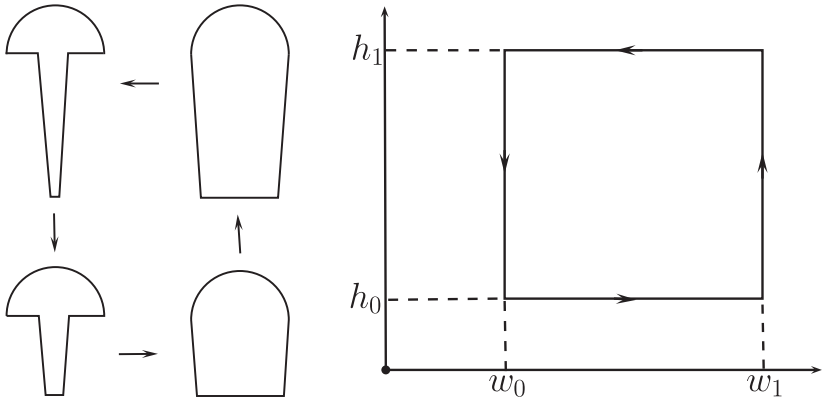

Figure 2. A cycle of the mushroom's oscillations: h and w are the length of the stem and its radius (half-width) at the cap respectively.

which connect the points

$$\left(w_1, h_1\right) \to \left(w_0, h_1\right) \to \left(w_0, h_0\right) \to \left(w_1, h_0\right) \to \left(w_1, h_1\right) \tag{23}$$

on the plane (w, h) while θ is fixed and $r = 1$ (see figure 2). For definiteness we assume that $w_0 < w_1$ and $h_0 < h_1$. The particle can be trapped inside the mushroom cap during the first stage of the process, when the hole shrinks, and then it is released during the third stage. Since the radius of the cap is fixed, the particle's energy stays constant while the particle remains in the cap.

The processes of capture and release are determined by the width of the gap: if the particle is captured into the cap at $t = t_{\text{in}}$ then it is released at $t = t_{\text{out}}$ such that $w(t_{\text{in}}) = w(t_{\text{out}})$. So we can rewrite equations (18) and (20)

$$\mathbb{E}\left[\log \frac{E_1}{E_0}\right] = \int_{w_0}^{w_1} (g(w) - 1 - \log g(w)) \mathrm{d}p_{\text{cha}}(w), \tag{24}$$

where

$$g(w) = \frac{V_{\text{cha}}\left(w, h_1\right)}{V_{\text{cha}}\left(w, h_0\right)} \qquad \text{and} \qquad p_{\text{cha}}(w) = \exp\left(- \int_w^{w_1} \frac{\mathrm{d}V_{\text{ell}}(w')}{V_{\text{cha}}\left(w', h_1\right)}\right),$$

and the volumes are defined by (1) and (2). In the derivation of the last equality we take into account that V_{cap} remains constant and $V_{\text{ell}} = \delta(w) V_{\text{cap}}$.

Then $p_{\text{nc}} = p(w_0)$ is the probability of avoiding the capture completely. If the particle avoids capture, equation (22) implies that the energy after a complete cycle is given by

$$\log \frac{E_1^{\text{nc}}}{E_0} = \int_{w_0}^{w_1} \left(\frac{1}{V_{\text{cha}}\left(w', h_1\right)} - \frac{1}{V_{\text{cha}}\left(w', h_0\right)} \right) \mathrm{d}V_{\text{ell}}(w'). \tag{25}$$

If a particle is captured at the moment when the hole size is w then its energy at the end of the cycle is described by (21), which takes the form

$$\log \frac{E_1(w)}{E_0} = \int_w^{w_1} \left(\frac{1}{V_{\text{cha}}\left(w', h_1\right)} - \frac{1}{V_{\text{cha}}\left(w', h_0\right)} \right) \mathrm{d}V_{\text{ell}}(w') + \log \frac{V_{\text{cha}}\left(w, h_0\right)}{V_{\text{cha}}\left(w, h_1\right)}. \tag{26}$$

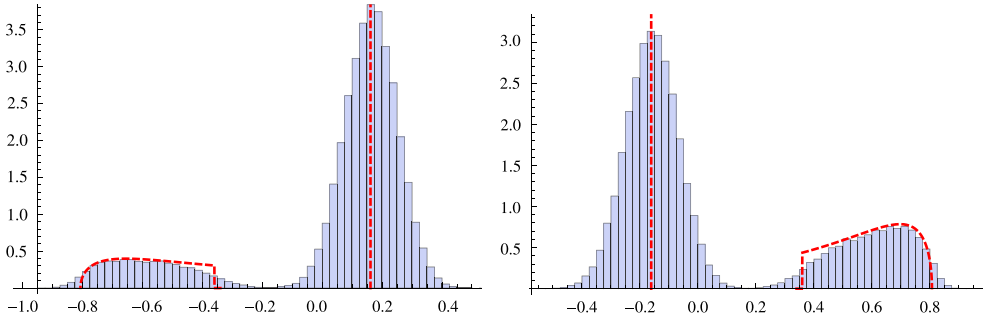

Figure 3. Distribution of $\log \frac{E_1}{E_0}$ for anticlockwise (left) and clockwise (right) protocols. The red dashed line represents the theoretical prediction. Parameters: $E_0 = 10^9$, $h_0 = 2$, $h_1 = 6$, $w_0 = 0.3$, $w_1 = 1$, $\theta = 2.3°$.

These equations can be used to construct a distribution for $\log \frac{E_1}{E_0}$ at the end of a cycle since they involve integrals of explicitly defined functions.

Another example is obtained when we reverse the protocol (23) by following the same path in the space of parameters in the clockwise direction

$$\big(w_1, h_1\big) \to \big(w_1, h_0\big) \to \big(w_0, h_0\big) \to \big(w_0, h_1\big) \to \big(w_1, h_1\big). \tag{27}$$

The distribution of the energy and the acceleration rate are described by the same equations but h_0 and h_1 are swapped.

In the first series of experiments we follow these two protocols by moving the billiard boundaries with piecewise constant acceleration. We generate $N = 10^5$ initial points uniformly distributed inside the billiard. All initial conditions have the same energy $E_0 = 10^9$ and a random direction of the initial velocity. Then we follow numerically the trajectory for each of the initial conditions during the time required to complete one cycle of the billiard boundary.

The distributions of the final energy E_1 is described by histograms which represent relative frequency density for $\log \frac{E_1}{E_0}$. The histograms are shown on figure 3 where the dashed red line represents the theoretical predictions for the energy distribution and the vertical red line marks the position of the theoretically predicted energy for non-captured particles. In parallel, we mark the capture and release time for each of the initial condition. In this way we test the accuracy of the theoretical prediction for the particle flux into the cap and, in particular, for $p_{\rm nc}$.

We see that the prediction for the energy growth rate is in good agreement with the numerically obtained average growth rate:

- **Anticlockwise protocol:** Theoretical prediction: $m_1 = \mathbb{E}[\log \frac{E_1}{E_0}] = 0.044926$. Non-captured particles: $\log \frac{E_1^{\rm nc}}{E_0} = 0.161205$ with probability $p_{\rm nc} = 0.843472$. Numerical simulations: average $m_1^* = 0.0463 \pm 0.0027$ for 10^5 initial conditions.
- **Clockwise protocol:** Theoretical prediction: $m_1 = \mathbb{E}[\log \frac{E_1}{E_0}] = 0.05252$. Non-captured particles: $\log \frac{E_1^{\rm nc}}{E_0} = -0.161205$ with probability $p_{\rm nc} = 0.717894$. Numerical simulations: average $m_1^* = 0.0537 \pm 0.0034$ for 10^5 initial conditions.

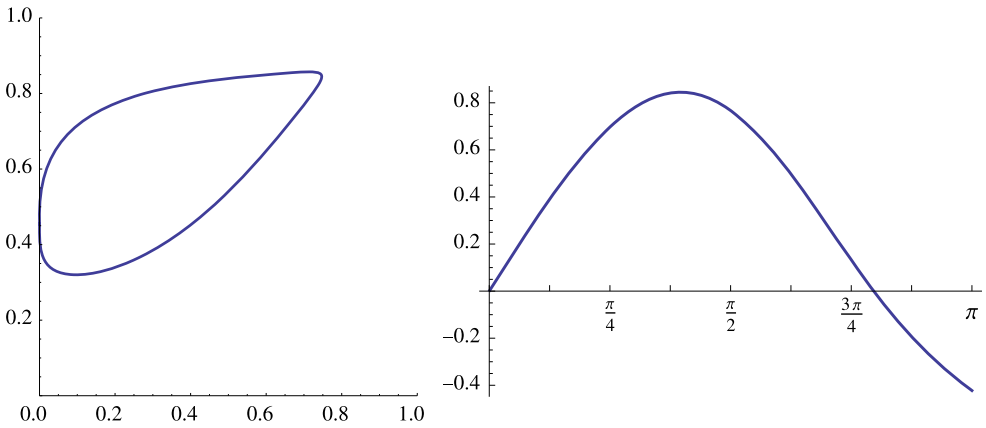

Figure 4. The cycle on the plane $\left(\frac{V_{\rm ell}(t)}{V_{\rm cap}(t)}, \frac{V_{\rm cap}(t)}{V(t)}\right)$ (clockwise direction). Parameters are $r_0 = h_0 = 1$, $a = 0.5$, $b = -0.5$, $c = 0.8$. On the right: theoretical prediction for $E_1(t_{\rm in})$ described by equation (21).

The histograms of figure 3 consist of two components which correspond to captured and non-captured particles. The distribution of the energy for the captured particles is apparently in good agreement with the theory. The distribution for the non-captured particles looks like Gaussian and its width scales as $E_0^{1/4}$. This behaviour has been observed for system where the ergodic averaging theory is applicable [7, 16]. The centre of the distribution is reasonably close to the value predicted by equation (25). We see that the proposed correction to the adiabatic theory (in particular, equation (22)) is realized. We also note that numerical experiments show that the relative frequency of escaping the capture is in excellent agreement with the theoretical prediction given by $p_{\rm nc}$. Notice that changing the loop direction leads to changing the role of heating in the stem and cap—clockwise motion means that the heating occurs in the cap and the cooling in the stem, whereas anticlockwise motion reverses their role. Yet, as predicted, the overall averaged growth rate of energy is positive in both cases.

4.2. Example with moving cap

In the second set of examples we change the billiard parameters in the following way

$$\begin{aligned} r(t) &= r_0 + a\,\sin(t), \qquad & w(t) &= r(t)\nu(t), \\ h(t) &= h_0 + b\,\sin(t), \qquad & \nu(t) &= 1 - c\,\sin^2(t). \end{aligned} \tag{28}$$

In this cycle all parameters of the billiard (except the slope θ) are changed simultaneously. The capture-release process is determined by $\nu(t) = \frac{w(t)}{r(t)}$. Since $\nu(t) = \nu(2\pi - t)$ for all t and ν is monotonically decreasing on $(0, \pi)$, there is a simple relation between the time of capture and the time of release

$$t_r(t) = 2\pi - t \qquad \text{for} \qquad t \in [0, \pi].$$

We find the compression factor from equation (18) and the energy growth rate from (20). Then the distribution of the energy after a complete cycle is found from equations (17), (21) and (22). For the purpose of plotting the distributions we evaluated these integrals numerically using the Simpson rule.

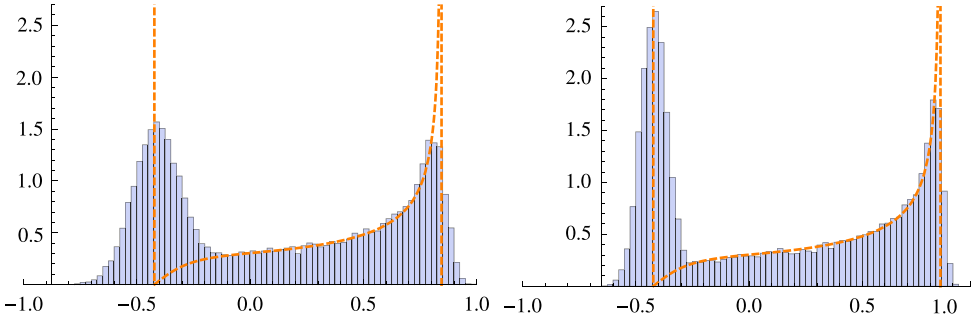

Figure 5. Distributions of $\log \frac{E_1}{E_0}$. Histograms are constructed on the basis of 25 000 initial conditions uniformly distributed inside the billiard. Initial velocity is taken with random direction, $E_0 = 10^6$ (left) and $E_0 = 10^7$ (right).

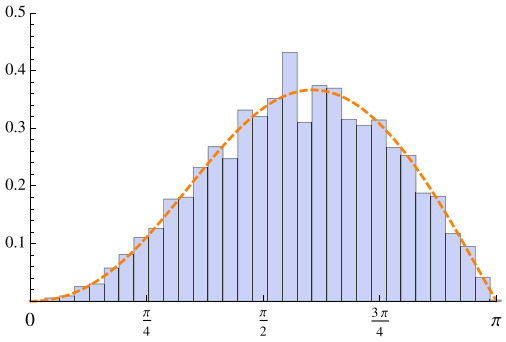

Figure 6. Distributions for times of capture

In the numerical experiments we use the following values for the parameters

$$r_0 = h_0 = 1, \qquad a = -0.5, \qquad b = 0.5, \qquad c = 0.8.$$

The slope of the billiard stem is kept equal to $\tan\theta = 0.1111$ during all experiments of the present section. The protocol is illustrated in figure 4. The right hand side plot shows the predicted energy after a full cycle for a particle captured at time $t_{\rm in}$, see equation (21). The positivity of energy gain for most of the captured particles corresponds to the right hump of the distribution shown in figure 5. The negative value for $t_{\rm in} = \pi$ implies that non-captured particles, on average, loose energy. A more accurate evaluation of the probabilities suggests $\log \frac{E_1^{\rm nc}}{E_0} = -0.422465$.

We select $N = 25\,000$ uniformly distributed initial conditions inside the billiard, which have the same initial energy and randomly chosen initial directions of velocity. The distribution of the energy after one cycle is shown on figure 5 for two selected values of the initial energy E_0. The dashed lines represent the theoretical distribution. We see that the numerical data are rather close to the theoretical prediction and, as it should be expected, the agreement is better for the higher initial energy. The distribution has two modes. The left mode corresponds to the particles which are not captured into the cap during the cycle. The position of the left mode is close to the theoretical prediction given by $\log \frac{E_1^{\rm nc}}{E_0} = -0.422465$

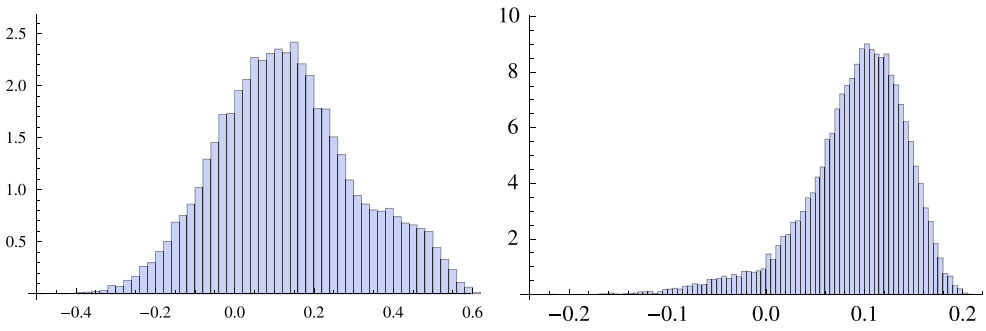

Figure 7. Distributions of $\frac{1}{10}\log\frac{E_{10}}{E_0}$ and $\frac{1}{30}\log\frac{E_{30}}{E_0}$. Histograms are constructed on the basis of 25 000 initial conditions uniformly distributed inside the billiard. Initial velocity is taken with random direction and $E_0 = 10^7$.

while the right mode corresponds to the maximum value of $\log\frac{E_1(t_{\rm in})}{E_0}$ (compare with figure 4 (right)).

The theoretical prediction for the growth rate is $m_1 = 0.122768$. During the numerical experiment with $E_0 = 10^7$ we obtain the average growth rate to be $m_1^* = 0.1213 \pm 0.0033$ ($\pm\,\sigma_N$) which is in excellent agreement with the theory. We also trace the capture and release times for each of the initial conditions. The distribution of the capture times is illustrated by a histogram shown on figure 6. The theoretical prediction obtained from equation (17) is plotted using the dashed line. In this experiment 38.78% of the particles are not captured in the cap, which is in a good agreement with the probability of non-capture being $p_{\rm nc} = 38.474\%$.

We conclude that the theory is overall in good agreement with the data from the numerical experiments, including both the distributions of energy and of capture time.

We see that after a single cycle the distribution of $\log\frac{E_1}{E_0}$ is quite far from being Gaussian. The central limit theorem suggest that if the increments of the logarithm of energy are not correlated over consecutive cycles, then the distribution of $\frac{1}{n}\log\frac{E_n}{E_0}$ should be close to the normal one centred around m_1 for large values of n. Figure 7 represents the distributions for $n = 10$ and $n = 30$. It is clearly seen that while the central part of the distribution is close to the predicted Gaussian shape, the tails apparently deviate from the normal distribution.

Finally, we stress that the non-ergodicity of the billiard plays the central role in the creation of the exponential acceleration. In order to illustrate this difference we consider a billiard cycle with the same parameters as above but setting $c = 0$. While the radius of the cap and the length of the stem are oscillating as in the previous experiments, the width of the stem coincides with the cap diameter and thus the frozen billiard table remains chaotic at all times. Here the ergodic adiabatic theory predicts that the energy should come to its initial value for the majority of the initial conditions. This is corroborated by a numerical experiment: the distribution of the energy after one cycle is shown in figure 8. We see that the final energy is distributed in a Gaussian-like way with quite small standard deviation: $|m_1^*| < 3 \cdot 10^{-5}$ and therefore we observe no exponential acceleration on average.

5. Summary and discussion

We propose a mechanism for achieving an averaged exponential acceleration rate for majority of initial conditions in a slowly varying system in which the fast dynamics have mixed phase

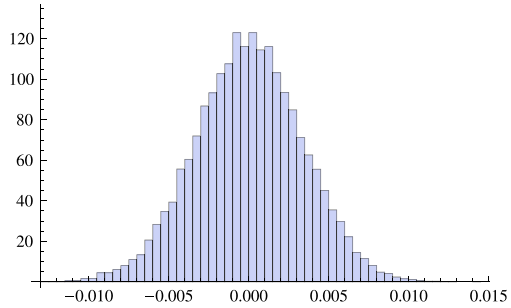

Figure 8. Distribution of $\log \frac{E_1}{E_0}$ for a chaotic billiard. Histograms are constructed on the basis of 25 000 initial conditions uniformly distributed inside the billiard. Initial velocity is taken with random direction and $E_0 = 10^7$. $a = 0.5$, $b = -0.5$, $c = 0$, $\tan\theta = 0.1111$.

space. The mechanism is examined by considering an oscillating Bunimovich mushroom, where analytical predictions are derived and are corroborated numerically. In particular, after finding explicit expressions for the volumes of the regular and chaotic components, we derive analytical expressions for the energy distribution after one cycle and for the exponential energy growth rates. Numerical experiments support our predictions for both the energy distribution and the growth rate, and support our claim that the violation of ergodicity is essential for getting exponential acceleration. We note that our mechanism does not require precise periodicity of the process—it only assumes that the billiard approximately restores its shape and size from time to time.

Our theory involves a generalization of the ergodic adiabatic theory which takes into account the flux between different ergodic components. We show that the averaged exponential growth rate is described by the following formula

$$m_1 := \mathbb{E}\left[\log \frac{E(T)}{E(0)}\right] = \int_{\text{capture}} (g - 1 - \log g)\mathrm{d}p_{\text{ell}}, \tag{29}$$

where g denotes the compression factor for the phase volumes between the moments of capture into the elliptic island and release (equation (18)) and p_{ell} denotes the probability of the particle being captured in the elliptic component. This formula is derived under quite general conditions and we hope that it may be applicable to other systems with mixed phase space.

Averaged exponential acceleration is achieved when the billiard parameters change along a non-trivial loop, for which the compression factor g of equation (29) is not identically one. A non-trivial loop bounds a non-empty interior when projected on a parameter plane in which one axis corresponds to the phase space volume of the chaotic zone and the other axis corresponds to the flux between the chaotic and integrable components. An important conclusion is that the exponential acceleration rate vanishes if the motion of the billiard boundary can be described by periodic oscillations of a single parameter (as is often done in numerical simulations of Fermi acceleration). Similarly, it vanishes if one of these two ingredients—the flux between the ergodic components or the volume change of the ergodic components—is missing. When the exponential rate vanishes, we still expect to observe some slow acceleration, typically quadratic in time (see e.g. [24, 25, 29, 30]).

We conjecture that the described mechanism, of exponential acceleration due to interior flux and volume changes for different ergodic components of systems with mixed phase space that are adiabatically deformed, is quite general. However, in contrast with the Bunimovich mushroom, in generic billiards and in generic smooth systems, the separation of the frozen fast system into ergodic components that depend continuously on parameters is more problematic. The existence of chaotic components with positive phase space volume is unknown, and the numerically observed boundary between the seemingly integrable and chaotic components is often 'sticky' and fractal. Nonetheless, we may envision that some rough estimates distinguishing the regular from the chaotic components may be derived (e.g. by calculating Lyapunov exponents), from which the compression rate g and the capture probability $p_{\rm ell}$ may be found. Then, formula (29) may formally connect these geometrical features of the frozen system with the energy growth rate in the adiabatically perturbed system. We should note that the influence of sticky or parabolic orbits on the statistics may be non-trivial. In fact, our initial numerical experiments with the classical Bunimovich mushroom, which has a rectangular stem and thus a family of parabolic periodic orbits, showed that the energy distribution in the chaotic zone was different from the one obtained with tilted geometry. The influence of these effects when multiple slow cycles are considered is yet to be explored.

While we do not anticipate that all the analytical predictions provided here may be carried over to the general case literally, we expect that the main principle, of achieving exponential acceleration by changing volumes of ergodic components on a non-trivial loop of parameters, is quite general.

Acknowledgements

This work is partially supported by EPSRC, the Leverhulme Trust, the Royal Society, and the Israel science foundation (Grant No. 321/12).

References

[1] Anosov D 1960 Averaging in systems of ordinary differential equations with rapidly oscillating solutions *(Russian) Izv. Akad. Nauk SSSR Ser. Mat.* **24** 721–42
[2] Arnold V I 1989 *Mathematical Methods of Classical Mechanics* (Berlin: Springer) doi:10.1007/978-1-4757-1693-1
[3] Arnold V I, Kozlov V V and Neishtadt A I 1988 Mathematical aspects of classical and celestial mechanics *Encyclopaedia of Mathematical Sciences* vol 3 (Berlin: Springer) pp 314–350
[4] Batistic B and Robnik M 2011 Fermi acceleration in time-dependent billiards: theory of the velocity diffusion in conformally breathing fully chaotic billiards *J. Phys.* A **44** 365101
[5] Batistic B 2014 Exponential Fermi acceleration in general time-dependent billiardsp 11 arXiv:1404.1747 [nlin.CD]
[6] Batistic B 2014 Fermi acceleration in chaotic shape-preserving billiards *Phys. Rev.* E **89** 022912
[7] Brown R, Ott E and Grebogi C 1987 The goodness of ergodic adiabatic invariants *J. Stat. Phys.* **49** 511–50
[8] Bunimovich L 1979 On the ergodic properties of nowhere dispersing billiards *Commun. Math. Phys.* **65** 295–312
[9] Bunimovich L 2001 Mushrooms and other billiards with divided phase space *Chaos* **11** 802–8
[10] Bunimovich L 2008 Chaotic and nonchaotic mushrooms *Discrete Contin. Dyn. Syst.* **22** 63–74
[11] Carvalho de R E, Souza F C and Leonel E D 2006 Fermi acceleration on the annular billiard *Phys. Rev.* E **73** 066229
[12] Carvalho de R E, de Souza F C and Leonel E D 2006 Fermi acceleration on the annular billiard: a simplified version *J. Phys.* A **39** 3561–73

[13] Dolgopyat D 2008 Fermi acceleration *Geometric and Probabilistic Structures in Dynamics* (*Contemporary Mathematics* vol 469) (Providence, RI: American Mathematical Society) pp 149–66
[14] Fermi E 1949 On the origin of the cosmic radiation *Phys. Rev.* **15** 1169–74
[15] Gelfreich V, Rom-Kedar V, Shah K and Turaev D 2011 Robust exponential acceleration in time-dependent billiards *Phys. Rev. Lett.* **106** 074101
[16] Gelfreich V, Rom-Kedar V and Turaev D 2012 Fermi acceleration and adiabatic invariants for non-autonomous billiards *Chaos* **22** 033116
[17] Gelfreich V and Turaev D 2008 Unbounded energy growth in Hamiltonian systems with a slowly varying parameter *Comm. Math. Phys.* **283** 769–94
[18] Gelfreich V and Turaev D 2008 Fermi acceleration in non-autonomous billiards *J. Phys. A: Math. Theor.* **41** 212003
[19] Gorelyshev I V and Neishtadt A I 2006 On the adiabatic perturbation theory for systems with impacts *J. Appl. Math. Mech.* **70** 4–17
[20] Itin A P and Neishtadt A I 2003 Resonant phenomena in slowly perturbed elliptic billiard *Regular and Chaotic Dyn.* **8** 59–66
[21] Kamphorst S O, Leonel E D and da Silva J K L 2007 The presence and lack of Fermi acceleration in nonintegrable billiards *J. Phys.* A **40** F887–93
[22] Karlis A K, Papachristou P K, Diakonos F K, Constantoudis V and Schmelcher P 2006 Hyperacceleration in a stochastic Fermi–Ulam model *Phys. Rev. Lett.* **97** 194102
[23] Kasuga T 1961 On the adiabatic theorem for the Hamiltonian system of differential equations in the classical mechanics *I, II, III, Proc. Japan Acad.* **37** 366–371, 372–376, 377–382
[24] Lenz F, Diakonos F K and Schmelcher P 2008 Tunable Fermi acceleration in the driven elliptical billiard *Phys. Rev. Lett.* **100** 014103
[25] Lenz F, Petri Ch, Diakonos F K and Schmelcher P 2010 Phase-space composition of driven elliptical billiards and its impact on Fermi acceleration *Phys. Rev.* E **82** 016206
[26] Liebchen B, Buechner R, Petri C, Diakonos F K, Lenz F and Schmelcher P 2011 Phase space interpretation of exponential Fermi acceleration *New J. Phys.* **13** 093039
[27] Llave de la R 2006 Some recent progress in geometric methods in the instability problem in Hamiltonian mechanics *Int. Congress of Mathematicians* vol 2 (Zurich: European Mathematical Society) pp 1705–29
[28] Lochak P and Meunier C 1988 Multiphase averaging for classical systems *With Applications to Adiabatic Theorems* (Berlin: Springer) p 360
[29] Loskutov A, Ryabov A B and Akinshin L G 2000 Properties of some chaotic billiards with time-dependent boundaries *J. Phys.* A **33** 7973–86
[30] Loskutov A and Ryabov A 2002 Particle dynamics in time-dependent stadium-like billiards *J. Stat. Phys.* **108** 995–1014
[31] MacKay R S 2010 Langevin equation for slow degrees of freedom of Hamiltonian systems *Nonlinear dynamics and chaos: advances and perspective* ed M Thiel *et al* (Berlin: Springer) pp 89–102
[32] Pereira T and Turaev D Exponential energy growth in adiabatically perturbed Hamiltonian systems in preparation
[33] Pustyl'nikov L D 1987 On the Fermi–Ulam model *Sov. Math. Dokl.* **35** 88–92
[34] Pustyl'nikov L D 1995 The existence of invariant curves for mappings that are close to degenerate and the solution of the Fermi–Ulam problem *Russ. Acad. Sci. Sb. Math.* **82** 231–41
[35] Shah K, Turaev D and Rom-Kedar V 2010 Exponential energy growth in a Fermi accelerator *Phys. Rev.* E **81** 056205
[36] Shah K 2011 Energy growth rate in smoothly oscillating billiards *Phys. Rev.* E **83** 046215
[37] Turaev D 2014 Exponential Fermi acceleration in adiabatically perturbed Hamiltonian systems *Proc. 8th European Nonlinear Dynamics Conference (ENOC)* p 2
[38] Ulam S M 1961 On some statistical properties of dynamical systems *Proc. 4th Berkeley Symp. Mathematical Statistics and Probability, Univ. California* vol 3 (Berkeley: University of California Press) pp 315–20